THE JOURNAL OF BIOLOGICAL CHEMISTRY VOL. 285, NO. 4, pp. 2506–2514, January 22, 2010

β-Amyloid Causes Depletion of Synaptic Vesicles Leading to Neurotransmission Failure*

Received for publication, June 8, 2009, and in revised form, November 11, 2009 Published, JBC Papers in Press, November 13, 2009, DOI 10.1074/jbc.M109.030023

Jorge Parodi[‡1,2], **Fernando J. Sepúlveda**[‡§1], **Jorge Roa**[‡], **Carlos Opazo**[§], **Nibaldo C. Inestrosa**[¶], **and Luis G. Aguayo**[‡‖3]

From the Laboratories of [‡]*Neurophysiology and* [§]*Neurobiometals, Department of Physiology, and* [‖]*Centro de Investigación Avanzada en Educación, University of Concepción, Edmundo Larenas S/N, P.O. Box 160-C, Concepción, Chile and* [¶]*Centro de Envejecimiento y Regeneración (CARE), Centro de Regulación Celular y Patología Joaquín V. Luco, Millenium Institute on Fundamental and Applied Biology, Facultad de Ciencias Biológicas, Pontificia Universidad Católica de Chile, Alameda 340, P.O. Box 114-D, Santiago, Chile*

Alzheimer disease is a progressive neurodegenerative brain disorder that leads to major debilitating cognitive deficits. It is believed that the alterations capable of causing brain circuitry dysfunctions have a slow onset and that the full blown disease may take several years to develop. Therefore, it is important to understand the early, asymptomatic, and possible reversible states of the disease with the aim of proposing preventive and disease-modifying therapeutic strategies. It is largely unknown how amyloid β-peptide (Aβ), a principal agent in Alzheimer disease, affects synapses in brain neurons. In this study, we found that similar to other pore-forming neurotoxins, Aβ induced a rapid increase in intracellular calcium and miniature currents, indicating an enhancement in vesicular transmitter release. Significantly, blockade of these effects by low extracellular calcium and a peptide known to act as an inhibitor of the Aβ-induced pore prevented the delayed failure, indicating that Aβ blocks neurotransmission by causing vesicular depletion. This new mechanism for Aβ synaptic toxicity should provide an alternative pathway to search for small molecules that can antagonize these effects of Aβ.

Alzheimer disease (AD)[4] is a progressive neurodegenerative brain disorder that leads to major debilitating cognitive deficits. It is believed that the cellular and molecular alterations capable of causing brain circuitry dysfunctions have a slow onset and that the full blown disease may take several years to develop (1). Therefore, it is important to understand the early, asymptomatic, and possible reversible states of the disease with the aim of proposing preventive and disease-modifying therapeutic strategies. The senile plaques found in the brain of patients with AD are characterized by insoluble peptides between 38 and 42 amino acids in length known as amyloid β-peptides (Aβ) (2). Previous studies have shown that the degree of cognitive impairment in patients with AD is not related to the insoluble form of the protein in the brain (3), and it was recently suggested that brain alterations might be more specifically associated with the synaptotoxic effects of soluble, oligomeric forms of Aβ (4).

It can be postulated that in its most incipient clinical form, the early symptoms of AD, confusion and loss of episodic and working memory, are due to network disconnections produced by oligomeric forms of Aβ (1). Therefore, in the context of a primarily synaptic disease, it is possible that this early form of brain dysfunction is similar to that induced by synaptically active drugs, such as benzodiazepines and ethanol (5). In agreement with this idea, aggregated Aβ can alter complex events in brain synaptic transmission, such as long term potentiation, which is believed to be essential for neuronal plasticity and learning phenomena (4, 6). More recently, Aβ dimers were found to inhibit long term potentiation, suggesting a large complexity on the nature of the neuroactive forms (7). Thus, it is now accepted that diverse forms of Aβ are responsible for producing synaptic failure, but how Aβ produces this malfunction is largely unknown.

It is known that Aβ oligomers, but not monomers, produce alterations in dendrite spine morphology in hippocampal neurons (4). Additionally, this structural change was associated with a decrease in the frequency of miniature excitatory postsynaptic currents and smaller effects on their amplitude. Also, Aβ caused NMDA receptor endocytosis without affecting the traffic of $GABA_A$ receptors in cortical neurons (8). Other studies, however, did not show effects of Aβ on NMDA neurotransmission, indicating some complexities (9). On the other hand, presynaptic proteins such as SNAP-25, synaptophysin, and synaptotagmin have also been reported to be reduced in brains of patients with AD and after treatment with Aβ (10, 11). Additionally, Aβ oligomers can alter dynamin-1, a neuron-specific mechanochemical GTPase that pinches off synaptic vesicles, allowing them to reenter the synaptic vesicle pool (12, 13).

Therefore, with the aim of shedding light on mechanisms associated with Aβ-induced synaptic failure in the brain, we examined the acute and chronic effects of Aβ aggregates, a mixture of protofibrils and oligomers (14, 15), on cultured hippocampal neurons. Our data show that low concentrations of Aβ produce inhibition of presynaptic function by causing calcium-dependent vesicular depletion. This novel mechanism might help us to develop new strategies to prevent and slow down the onset of the disease.

* This work was supported by Fondo Nacional de Desarrollo Cientifico y Technologico Grant 1060368, Ring of Research Programa Bicentenario de Ciencia y Tecnologia ACT-04, CIE-05 (to L. G. A. and C. O.) and Direccion de Investigacion Universidad de Concepcion Grant 205.033.101-1.0 (to J. R.).

[1] Both authors contributed equally to this work.

[2] Present address: Laboratorio de Neurociencias-CEBIOR, Universidad de la Frontera, Temuco, Chile.

[3] To whom correspondence should be addressed: Dept. of Physiology, University of Concepción, P.O. Box 160-C, Concepción, Chile. Tel.: 56-41-220-3380; Fax: 56-41-224-5975; E-mail: laguayo@udec.cl.

[4] The abbreviations used are: AD, Alzheimer disease; Aβ, amyloid β-peptide; AMPA, α-amino-3-hydroxy-5-methyl-4-isoxazolepropionic acid; CNQX, 6-cyano-7-nitroquinoxaline-2,3-dione; $GABA_A$, γ-aminobutyric acid type A; NMDA, *N*-methyl-D-aspartic acid; RRP, readily releasable pool.

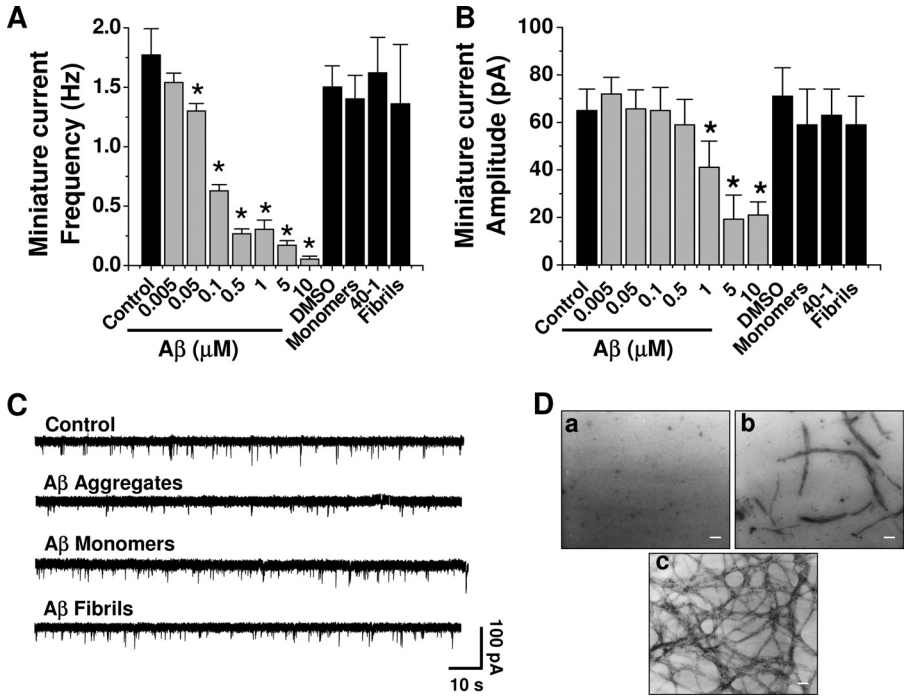

FIGURE 1. **Inhibition of synaptic transmission by nanomolar Aβ.** *A* and *B*, hippocampal neurons were exposed to different concentrations of Aβ for 24 h. Soluble fibrils and reverse (1 μM) peptides were also examined on frequency and amplitude of miniature currents. The *bars* are mean ± S.E. from 16 different neurons (*, $p < 0.05$). *DMSO*, dimethyl sulfoxide. *C*, typical miniature synaptic currents obtained under different aggregation states. *D*, electron micrographs showing three states of Aβ aggregation (all at 80 μM): monomers (fresh solution) (*a*), mixture of aggregates (obtained after 120 min of aggregation) (*b*), and fibrils (obtained after 72 h of aggregation) (*c*). *Scale bars*, 50 nm.

EXPERIMENTAL PROCEDURES

Hippocampal Cultures—Hippocampal neurons were obtained from 18-day-old mice embryos as described previously (16) in accordance with National Institutes of Health recommendations. The neuronal feeding medium consisted of 90% minimal essential medium (Invitrogen), 5% heat-inactivated horse serum, 5% fetal bovine serum, and a mixture of nutrient supplements. All animals were handled in strict accordance with National Institutes of Health recommendations, and all animal work was approved by the appropriate committee at the University of Concepción.

Aβ Aggregation—Both human synthetic $Aβ_{1-40}$ (wild-type) and $Aβ_{40-1}$ (reverse sequence) peptides (Tocris Bioscience, Ellisville, MO) were dissolved in dimethyl sulfoxide at a concentration of 10 mg/ml and immediately stored in aliquots at −20 °C. 25 μl of stock solution was diluted to a final concentration of 80 μM in 725 μl of phosphate-buffered saline (GIBCO) and stirred continuously (200 rpm) at 37 °C. The formation of aggregates was monitored by turbidity measurements ($A_{405\ nm}$) and stored at 4 °C until use.

Patch Clamp Recordings—Patch pipettes (1–3 MΩ) were prepared from filament-containing borosilicate micropipettes. Acute applications of Aβ were done with a mobile series of pipettes (approximately 200 μm in diameter). Currents were measured with the whole cell patch clamp technique at a holding potential of −60 mV using an Axopatch 200B amplifier (Axon Instruments). The data were displayed and stored using a 1322A Digidata acquisition board and analyzed with electrophysiological software (Axon Instruments). The external solution contained 150 mM NaCl, 5.4 mM KCl, 2.0 mM $CaCl_2$, 1.0 mM $MgCl_2$, 10 mM glucose, and 10 mM HEPES (pH 7.4, 330 mOsmol). The standard internal solution in the patch pipette contained 120 mM KCl, 4.0 mM $MgCl_2$, 10 mM BAPTA, and 2.0 mM Na_2-ATP (pH 7.4, 310 mOsmol). Some studies involved the use of external solutions without calcium (10 μM by atomic absorption) or Na7 (100 μM). For longer incubations, Aβ was diluted in the culture medium to a final working concentration in the absence or presence of 1 mM EGTA (for low calcium solution) or with Na7, Na13, or Na15 (100 μM; AnaSpec, Fremon, CA). Evoked membrane currents were obtained by local application of 100 μM AMPA using a series of glass flow pipettes fed by gravity. The data are presented normalized to cell capacitance. Analysis of cell capacitance was done with ClampFit software using a 5-mV depolarizing pulse. Spontaneous postsynaptic currents were recorded in 2-min segments. $GABA_A$ neurotransmission was isolated pharmacologically in the presence of 2 μM CNQX. The currents were blocked by 4 μM bicuculline. To isolate AMPA currents pharmacologically, the external solution contained 4 μM bicuculline and 2 mM Mg^{2+}. The release of the readily releasable pool (RRP) was achieved using a hyperosmotic external solution (500 mOsm/liter sucrose). The data were analyzed with the MiniAnalysis 8.0 program (Synaptosoft, Inc., Leonia, NY) to obtain mean averages of peak amplitude, frequency, and decay time constant (between 90 and 10% of decay). Amplitude histograms were plotted with a bin width of 2–5 pA. From the resulting data, cumulative or frequency histograms were generated.

Western Blotting—Standard Western blotting procedures were used (13). Equal amounts of protein were separated on 10–12% SDS-polyacrylamide gels. Protein bands were transferred onto nitrocellulose membranes, blocked with 5% nonfat milk, and incubated with primary antibodies using the following concentrations: 1:500 anti-dynamin-1 (Chemicon, Temicula, CA), 1:500 anti-synapsin-1 (Chemicon), 1:500 anti-synaptophysin (Zymed Laboratories), 1:1000 anti-SV2 (Developmental Studies Hybridoma Bank, Iowa City, IA), 1:2000 anti-α-tubulin (Sigma), 1:500 anti-syntaxin-1 (Chemicon), 1:500 anti-GluR1 (Chemicon), 1:500 anti-NR1 (Chemicon), 1:1000 anti-PSD-95 (Affinity Bioreagents), and 1:500 anti-α1-$RGABA_A$ (Santa Cruz Biotechnology, Santa Cruz, CA). Bands were visualized with the ECL Plus Western blotting detection system (PerkinElmer).

Calcium Imaging—Neurons were loaded with Fluo-3 AM (1 μM in pluronic acid/dimethyl sulfoxide; Molecular Probes)

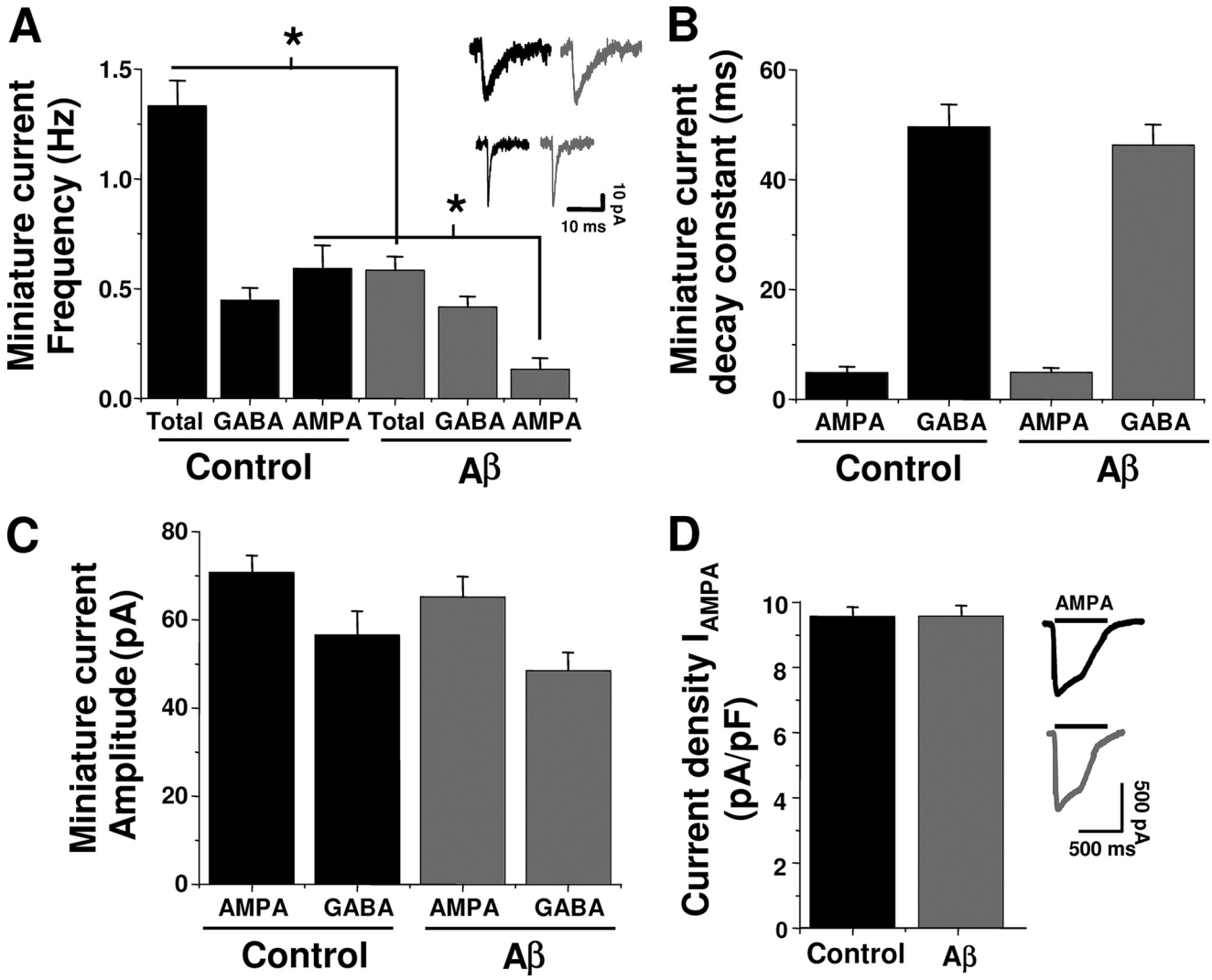

FIGURE 2. **Effect of Aβ on glutamatergic and GABAergic transmissions.** *A*, Aβ (500 nM, 24 h) on frequency of total and isolated AMPA and $GABA_A$ miniature currents. *Insets*, characteristic $GABA_A$ (*upper*) and AMPA (*lower*) currents. *B* and *C*, effects of Aβ on time course and peak amplitude of postsynaptic currents. *D*, current density for evoked AMPA responses in control and Aβ-treated neurons. The *symbols* are mean ± S.E. from at least five neurons (*, $p < 0.05$).

for 30 min at 36 °C. The neurons were then washed twice with external solution and incubated for 30 min at 36 °C. The cells were mounted in a perfusion chamber that was placed on the stage of an inverted fluorescent microscope (Eclipse TE; Nikon) equipped with a xenon lamp and a ×40 objective (22–24 °C). The cells were briefly illuminated (200 ms) using a computer-controlled Lambda 10-2 filter wheel (Sutter Instruments). Regions of interest were simultaneously selected on neuronal somata containing Fluo-3 fluorescence (excitation 480 nm, emission 510 nm) in an optical field having usually more than 10 cells. Images were collected at 2–5-s intervals during a continuous 5-min period. The imaging was carried out with a 12-bit cooled SensiCam camera (PCO, Kelheim, DE).

FM1-43 Loading and Unloading—Presynaptic vesicles were labeled by exposure to styryl dye FM1-43 (15 μM; Molecular Probes) during a high K^+ depolarization for 5 min and washed immediately. Coverslips were mounted on a rapid switching flow perfusion chamber with an epifluorescence microscope (Nikon Eclipse 3000). Depolarization-dependent destaining was induced by bath perfusion with 30 mM K^+ (equiosmolar replacement of Na^+). To measure the effect of Aβ on post-stimulus endocytosis, control and treated neurons were stimulated for 5 min in 30 mM K^+ and exposed to FM1-43 for 5 min after a variable delay (Δt) from the onset of the stimulus. As the Δt increased, the endocytosis cycle was completed, reducing actual FM1-43 uptake (17). The reduced endocytosis was expressed relative to that of $\Delta t = 0$.

Immunofluorescence—Presynaptic terminals were loaded with AM1-43 (15 μM; Biotium, Inc., Hayward, CA) during high K^+ depolarization for 5 min and immediately washed in dye-free solution with nominal Ca^{2+} to minimize spontaneous dye loss, fixed for 30 min with 4% paraformaldehyde, and permeabilized with 0.1% Triton X-100 in phosphate-buffered saline. Nonspecific immunoreactivity was blocked with 10% horse serum for 1 h at room temperature. Monoclonal synapsin-1 antibody (1:100; Santa Cruz Biotechnology) was incubated overnight followed by incubation with an anti-goat secondary antibody conjugated with fluorescein isothiocyanate (1:500; Jackson ImmunoResearch Laboratories).

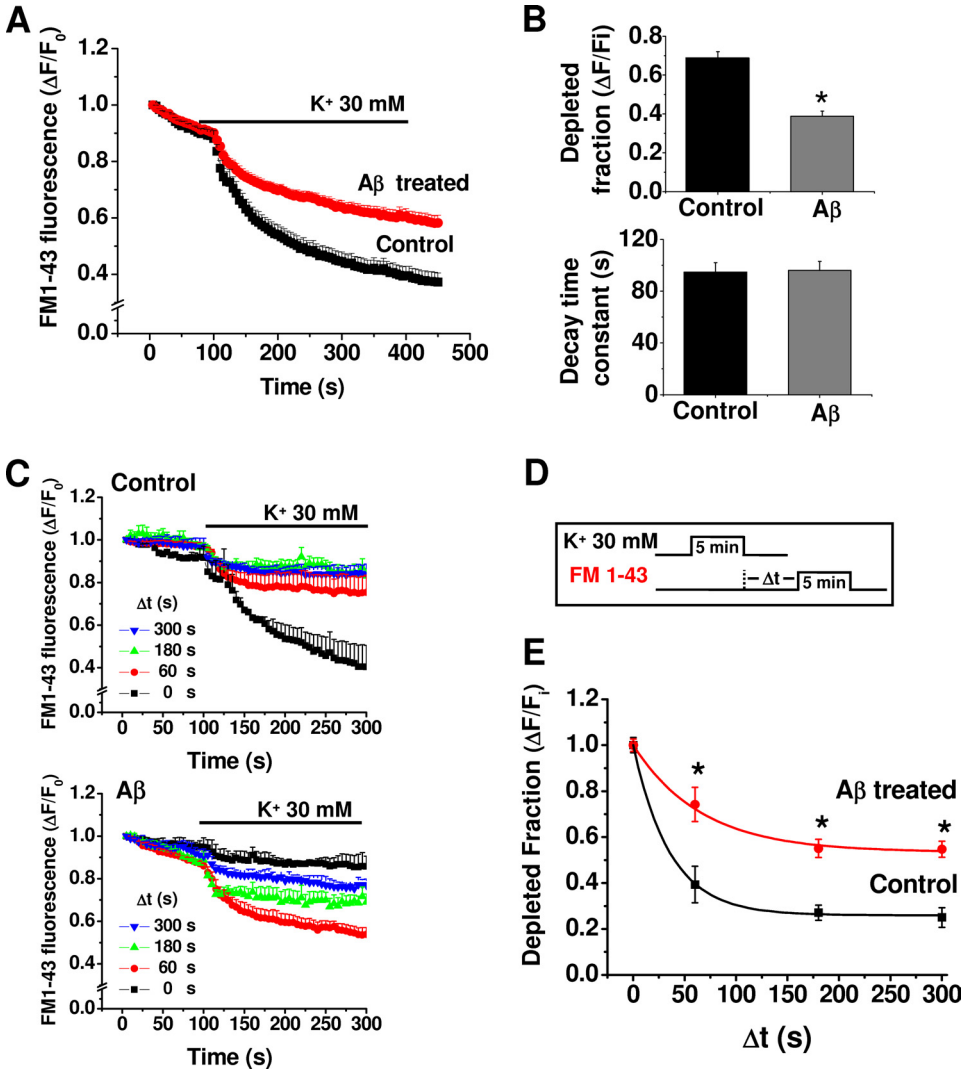

FIGURE 3. **Aβ reduced synaptic vesicle recycling.** *A*, K^+-induced destaining of FM1-43 in control and Aβ-treated neurons. *B*, effect of Aβ (500 nM, 24 h) on fractional and time constant of FM1-43 release. *C*, ratio of endocytosis of FM1-43 following a variable time delay (0–300 s) from an initial depolarizing K^+ pulse in control and treated neurons. *D*, protocol used to load FM after variable times of exocytosis. *E*, time course of FM1-43 fluorescence constructed from the data in *C* for control and treated neurons. The *lines* are the best single-exponential fit to the data. The *symbols* are mean ± S.E. from 12 independent recordings (*, $p < 0.05$).

The samples were mounted in fluorescent mounting medium (DAKO) for confocal analysis.

Fluorescence Measurements and Confocal Microscopy—FM1-43 immunofluorescence was acquired using an epifluorescence Nikon microscope (Eclipse TE; Nikon) equipped with a ×100 objective (Neofluor, oil immersion, NA 1.0). FM1-43 fluorescence was excited at 540 nm and collected with 620-nm long pass filters. Fluorescence intensity was measured using a 2 × 2 binning with a CCD camera (SensiCam; PCO). Images were digitized and processed with Imaging Axon Workbench 2.2 (Axon Instruments). AM1-43 and fluorescein isothiocyanate immunofluorescence were visualized using a confocal Nikon C1 TE2000U microscope (×60, water immersion, NA 1.4) with lasers of argon (488 nm) and He-Ne (543 nm) for fluorescein isothiocyanate and AM1-43, respectively. After acquisition, images were processed with ImageJ (National Institutes of Health). Co-localized punctas in the soma and primary processes (50 μm) were counted for control and treated neurons.

Transmission Electronic Microscopy—Samples of 20 μl of Aβ, at a concentration of 50 μM, were applied to carbon-coated Formvar grids (ORIGEN) pretreated with glutaraldehyde solution. Amyloid fiber or aggregates were stained with 20 μl of 2% (w/v) uranyl acetate solution, and the grid was air-dried. Samples were examined using a JEOL 1200 EX II electronic microscope. In other experiments, neurons plated directly onto the bottom of 35-mm plastic tissue culture plates were used. Cultures of 12 days *in vitro* neurons were incubated with Aβ for 24 h, subsequently washed, and then fixed for 30 min with 2% glutaraldehyde. The samples were placed in a plastic resin, sectioned, and mounted on a grid. The samples were visualized on a Phillips electronic microscope (model EM-300) operated between 60 and 120 kV. Using a double-blind protocol, synaptic boutons from control and Aβ-treated neurons were counted. Here, all sections were analyzed in codified samples. Only at the end of the experiment were the sections identified as part of an experimental condition. The number of synaptic vesicles was counted in the area that included the high electron dense postsynaptic zone.

Data Analysis—Nonlinear analysis was performed using Origin (Microcal). The values are expressed as mean ± S.E. Statistical differences were determined using Student's *t* test or analysis of variance. The experiments were performed in triplicate.

RESULTS

Effects of Chronic Aβ on Synaptic Transmission in Hippocampal Neurons—Previous studies have shown that Aβ inhibits synaptic transmission in brain neurons (6, 18, 19). Those studies suggested that the inhibition was due to a postsynaptic action because Aβ reduced long term potentiation and excitatory postsynaptic current amplitudes. However, only a single concentration of Aβ (usually 1 μM) and one time point were analyzed, making it difficult to determine the mechanisms and kinetics of the inhibition. To gain further insights on potential differences at a range of concentrations, hippocampal neurons were exposed for 24 h to several concentrations of Aβ (5 nM–10 μM). A low concentration of Aβ (5 nM) was without effect on synaptic transmission parameters. In contrast, higher con-

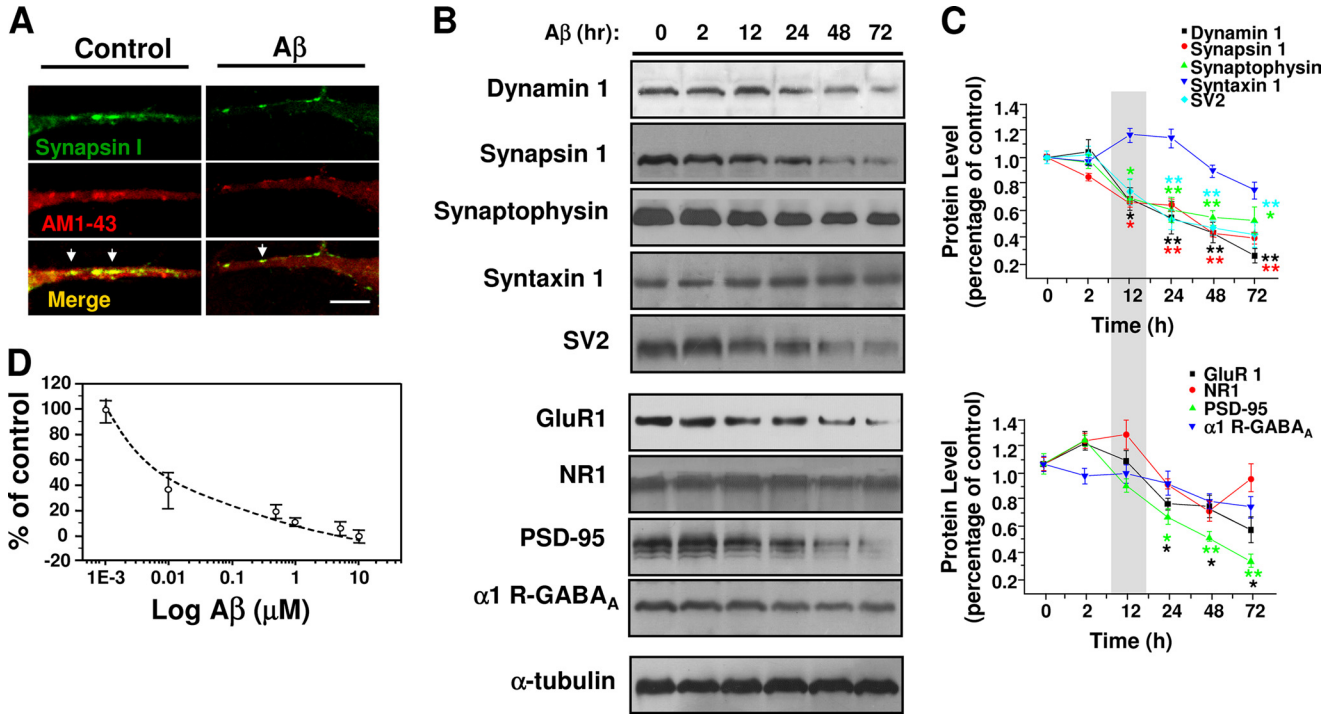

FIGURE 4. **Aβ reduced several synaptic vesicle proteins.** *A*, confocal micrographs showing the effect of chronic Aβ (500 nM, 24 h) on active synaptic proteins visualized by co-localization of synapsin-1 and AM1-43 (*yellow* and *arrows*). *B*, time course of Aβ effects on the level of several pre- and postsynaptic proteins. *C*, graphs showing the quantification of signal intensity obtained at different times of treatment. The faster effect of Aβ at 12 h was on presynaptic proteins. The *bars* are mean ± S.E. from three independent experiments (*, $p < 0.05$; **, $p < 0.01$).

centrations (50–500 nM) reduced the frequency of miniature currents, without manifesting changes in amplitude (Fig. 1, *A* and *B*). Aβ decreased quantal current amplitude at concentrations of 1 μM and above (Fig. 1*B*). On the other hand, neurons exposed to Aβ monomers, fibrils, or reverse $Aβ_{40-1}$ (all at 500 nM) displayed unchanged neurotransmission (Fig. 1*C*). The ultrastructural forms (oligomers and short fibrils) that appeared after 120–150 min of agitation, corresponding to the neuroactive Aβ forms, were structurally (Fig. 1*Db*) and functionally similar to a heterogeneous array of forms defined as oligomers, protofibrils, and Aβ-derived diffusible ligands, known to enhance neuronal spiking and intracellular calcium (14, 20, 21). These features were not observed in either nonaggregated peptide (monomers) (Fig. 1*Da*) or in aggregated peptides after 3 days of incubation, where long mature fibrils were mainly observed (Fig. 1*Dc*). Therefore, the neuroactive forms of Aβ able to depress synaptic transmission corresponded to intermediate aggregates.

Under the present experimental conditions, the predominant glutamatergic transmission was AMPAergic, whereas the inhibitory transmission was GABAergic. Few low amplitude synaptic NMDA currents were detected in our recordings, and because of conflicting effects of Aβ on this receptor (4, 22), we decided to focus the present study mainly on pharmacologically isolated AMPA and $GABA_A$-mediated synaptic currents. The inhibitory effect of chronic Aβ was highly selective for glutamatergic transmission because the miniature GABAergic currents were not significantly altered (Fig. 2*A*). On the other hand, analyses of the peak current amplitude and time constant of decay, parameters related to the postsynaptic responsiveness to neurotransmitters, showed that AMPA and $GABA_A$ receptors were affected to a lower extent (Fig. 2, *B* and *C*). Furthermore, direct application of 100 μM AMPA to the postsynaptic membrane (Fig. 2*D*) and analysis of cumulative probability of AMPA synaptic currents in control and treated neurons (not shown) showed that the current density was unchanged by 24 h of Aβ incubation suggesting that membrane levels of AMPA receptors were not affected.

Effects of Aβ on Vesicular Recycling in Hippocampal Neurons—To monitor directly whether the decrease in miniature excitatory postsynaptic current frequency was related to changes in exocytosis-endocytosis vesicular cycles, we performed cellular imaging with FM1-43 (23, 24, 17). Application of 30 mM external K^+ indicated that the destaining (exocytosis) of FM1-43 was significantly reduced by chronic application (24 h) of 500 nM Aβ (Fig. 3*A*). Additional experiments using AM1-43, a fixable form of FM1-43, showed that the vesicular uptake was reduced by more than 40% with chronic Aβ (95 ± 5 *versus* 55 ± 5 arbitrary fluorescent units, $n = 3$). Moreover, although the level of released FM1-43 was reduced by Aβ, the time constant of exocytosis was similar (Fig. 3*B*). Next, we examined the capacity of the stimulated vesicles to reuptake the fluorescent dye to determine whether endocytosis was being altered by Aβ. Using a modified FM1-43 reuptake protocol (17), we found that control vesicles completed ~80% of the dye endocytosis within 60 s of the depolarizing stimuli (Fig. 3, *C* and *D*), with a time constant for endocytosis of 35 ± 5 s (Fig. 3*E*), which is in agreement with previous studies (17). Aβ caused a lengthening of the time constant of this process (66 ± 6 s). Therefore, the data showed that a low concentration of Aβ reduced the magnitude of exocytosis and that the remaining synaptic vesicles displayed a much slower speed of endocytosis.

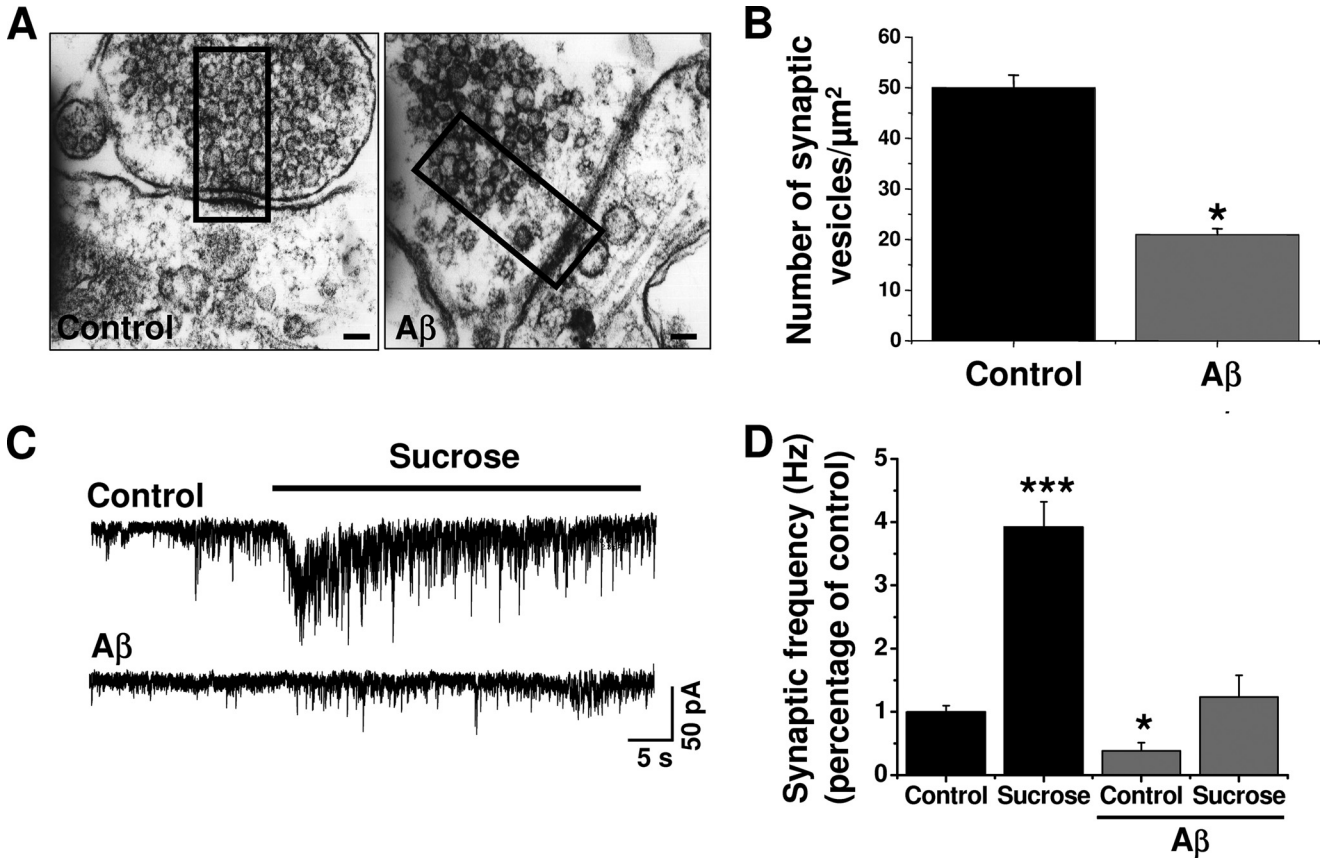

FIGURE 5. **Aβ reduced the synaptic vesicular pool.** *A*, electron micrographs show synapses from control (*left*) and 500 nM Aβ-treated (*right*) neurons. *Rectangles* illustrate the areas for quantification. *Scale bars*, 100 nm. *B*, columns showing the number of vesicles in both conditions from 12 selected active zones using a double-blind protocol (*, $p < 0.05$). *C* and *D*, effect of hypertonic sucrose solution (500 mOs) on miniature current frequencies in control and Aβ (500 nM)-treated neurons. *Bars* are mean ± S.E. from 18 neurons (***, $p < 0.001$; *, $p < 0.05$).

Early Effects of Aβ on Presynaptic Proteins—Confocal microscopy showed a reduction in active synaptic vesicles in Aβ-treated neurons. This was shown as a diminished co-localization of synapsin-1 and the FM1-43 fixable analog AM1-43, expressed by the number of presynaptic puncta/10-μm length (Fig. 4, *A* and *D*). In addition, quantitative analyses of several presynaptic proteins showed that with the exception of syntaxin-1 they were all reduced with 12 h of treatment with Aβ, partly explaining the synaptic failure. On the other hand, among the postsynaptic proteins, only PSD-95 and GluR1 levels were significantly altered at 24 h with Aβ (Fig. 4*B*). These data indicate that the low Aβ concentration induced an earlier presynaptic deficit, which was followed by a postsynaptic alteration. The lack of functional differences (Fig. 2*D*) suggests that under this condition (time and concentration) active AMPA membrane receptors were still basically normal.

Previous experiments suggested that Aβ reduced several presynaptic proteins (12, 25, 26). Therefore, we decided to examine the ultrastructural features of the synapses using electron microscopy in double-blind experiments. The data showed that neurons cultured with Aβ displayed a reduced number of synaptic vesicles, especially those near the presynaptic active zones (Fig. 5*A*). Quantitative analysis showed that the number of synaptic vesicles was reduced from 50 ± 4 vesicles/μm^2 in control to 18 ± 3 vesicles/μm^2 in Aβ-treated neurons (Fig. 5*B*). These data suggest that chronic application of Aβ might affect the RRP of synaptic vesicles. To test this possibility further, we studied the synaptic transmission induced by a hyperosmotic sucrose solution, known to cause the release of RRP (27, 28). These experiments showed that unlike control neurons (*top trace*, Fig. 5*C*), which had a 4-fold increase in synaptic currents in the hypertonic solution (Fig. 5*D*), the Aβ-treated neurons had few miniature synaptic currents (Fig. 5*D*), and their frequency was less affected by the hypertonic solution.

Acute Aβ Increased Intracellular Calcium, Vesicle Release, and Synaptic Transmission—Aβ was shown to increase intracellular calcium in non-neuronal cells (21, 22). In agreement, short (60-s) applications of Aβ (500 nM–5 μM) with a puffer pipette induced a rapid and reversible increase in intracellular calcium in hippocampal neurons (Fig. 6*A*). It seemed feasible that this increase in intracellular calcium could affect the discharge of synaptic vesicles (29). We found that Aβ perfusions (500 nM–5 μM, 30 min) produced a concentration-dependent increase in miniature current frequency (Fig. 6*B*). Parallel analysis of FM1-43 destaining in the presence of Aβ (500 nM) showed enhancement in the slope of fluorescent decay ($-1.2 \times 10^{-4} \pm 3.0 \times 10^{-6}$ *versus* $-3.3 \times 10^{-4} \pm 3.2 \times 10^{-6}$ URF/s; $p < 0.0001$) after 10 min of application (Fig. 6*C*).

The above mentioned results showed that a short application (30 min) of Aβ increased the frequency of miniature synaptic currents in the neurons, whereas longer exposures (24 h) reduced it (Figs. 1*A* and 6*C*). Therefore, we decided to examine

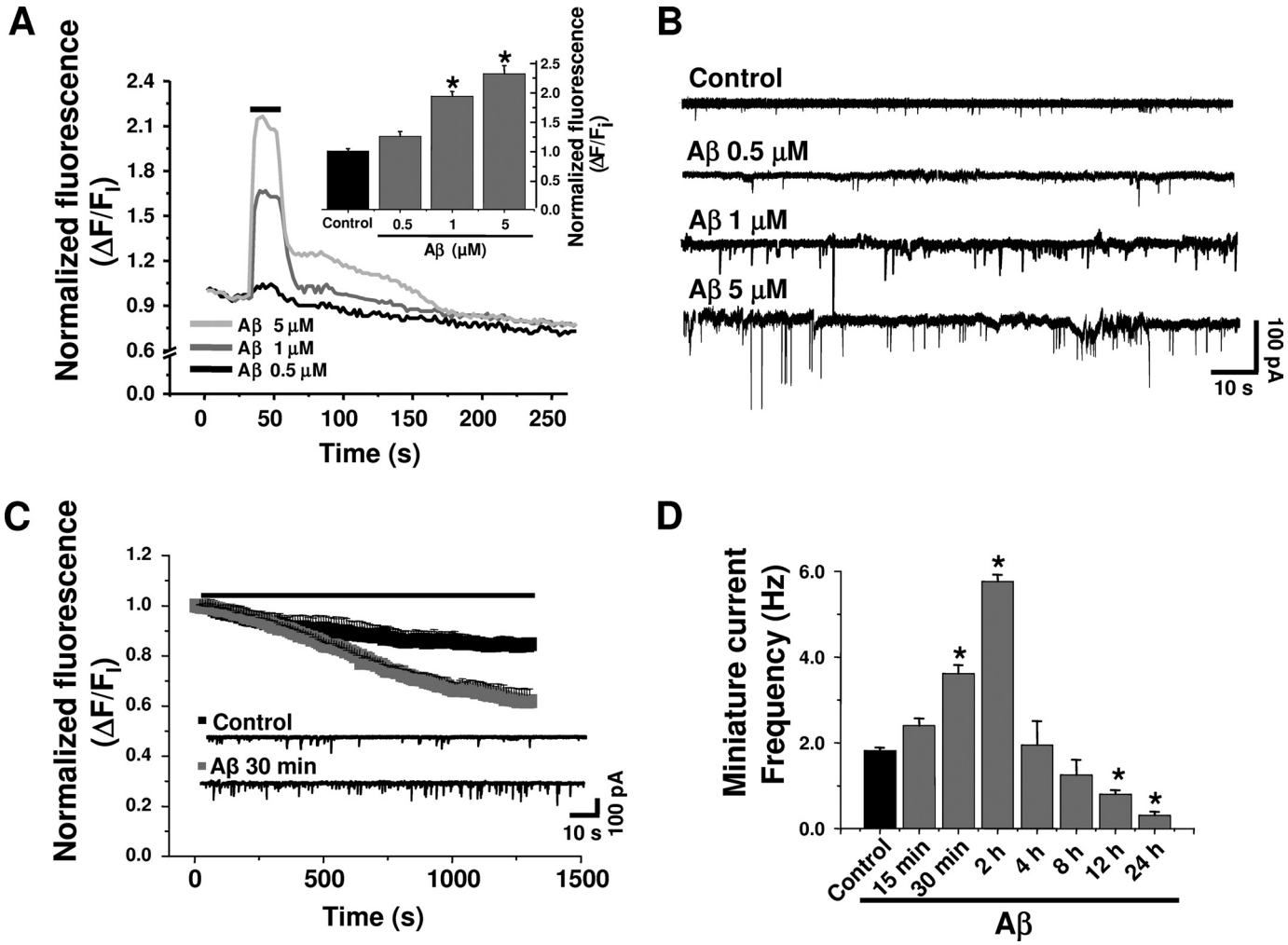

FIGURE 6. **Acute Aβ increased intracellular calcium and the release of synaptic vesicles.** *A*, Fluo-3-associated fluorometric recordings showing increases in intracellular calcium produced by short applications of Aβ (500 nM–5 μM). *Inset*, concentration-dependent effects of Aβ on intracellular calcium from three independent experiments ($p < 0.05$). *B*, traces showing the rapid increase in miniature synaptic current frequency with different concentrations of Aβ. *C*, FM1-43 destaining under control (*filled symbols*) and Aβ containing solutions (*open symbols*). The current traces were obtained after 30 min of exposure to control and 500 nM Aβ. *D*, effect of different Aβ incubation times on the frequency of miniature synaptic currents. *Bars* are mean ± S.E. from at least six neurons (*, $p < 0.05$).

the effects of Aβ on synaptic transmission after exposing the neurons to Aβ for various times (15 min up to 24 h). The data showed that the frequency of miniature currents was greatly increased during the first 2 h, and thereafter the frequency decreased progressively to well below the control level (Fig. 6*D*). The results mentioned above suggest that the synaptic failure produced by the prolonged action of Aβ on the synapse may be due to the strong early enhancement of quantal transmitter release leading to neurotransmitter vesicle depletion. Before testing this hypothesis, it was relevant to determine the mechanism by which Aβ enhanced intracellular calcium and synaptic release. Given that the increase in intracellular calcium could be mediated by voltage-dependent calcium channels (30), glutamatergic receptors (NMDA and AMPA) (8, 31), or amyloid pores (32), we studied the action of several inhibitors. Analysis of Aβ-induced increase in intracellular calcium, monitored with Fluo-3, showed that it was not blocked by a mixture containing calcium channel antagonists (ω-conotoxin, agatoxin-VI, and nifedipine) or CNQX and AP5 ((2*R*)-amino-5-phosphonopentanoate), antagonists of AMPA and NMDA receptors, respectively. Next, we used a small seven-amino acid peptide (Na7) that has been shown to block the ion current induced by Aβ amyloid pores in lipid membranes, as well as Aβ cellular toxicity (33, 34). Interestingly, this peptide blocked most of the increase in intracellular calcium induced by Aβ (Fig. 7*A*), suggesting that the calcium increase was mediated by the formation of amyloid pores in the neuronal membrane. In agreement with the involvement of a calcium-dependent mechanism on the acute and long term effects of Aβ on synaptic transmission, we found that its early and chronic synaptic effects were blocked by reducing extracellular calcium (from 2 to 0.01 mM) or by adding Na7 (Fig. 7*B*). Na7 also antagonized the Aβ-induced decrease in SV2 (Fig. 7*C*). Two analogs (Na13 and Na15) previously reported to be inactive blocking the ion permeation through the Aβ pore were not able to antagonize Aβ actions on a presynaptic marker (Fig. 7, *C* and *D*), emphasizing the role of calcium influx through the amyloid pore in synaptic failure. Additionally, these data support the critical role proposed for the histidines in Na7 (33).

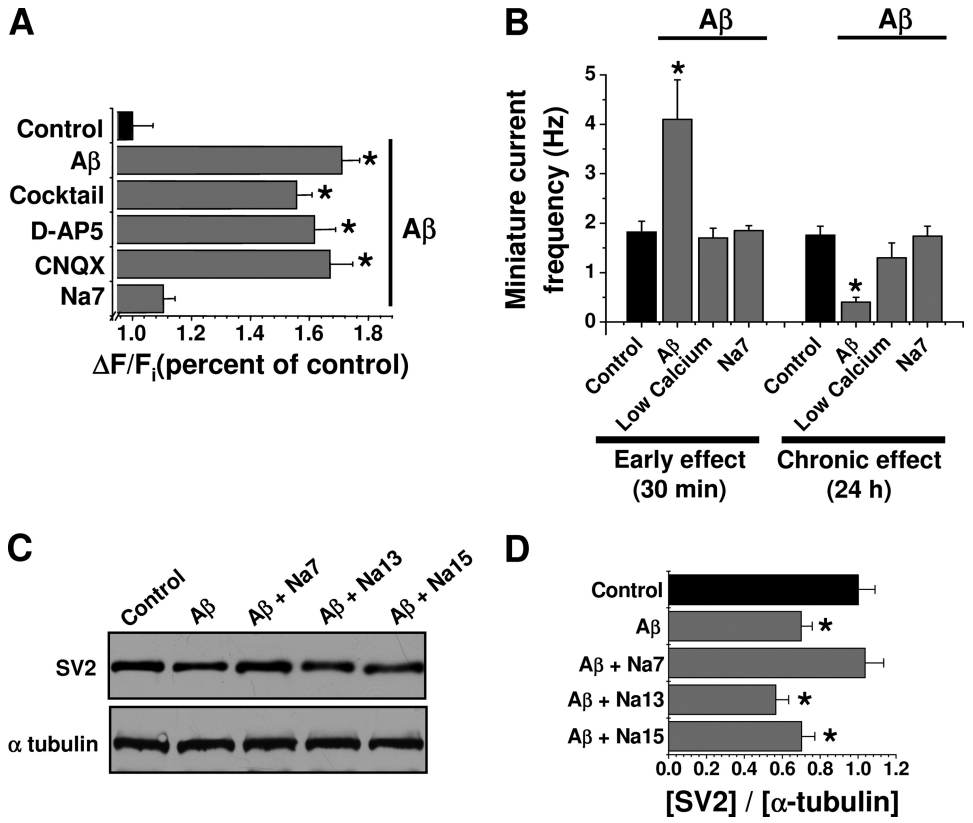

FIGURE 7. **Blockade of Aβ induced increases in intracellular calcium and synaptic transmission by a small peptide.** *A*, effect of several calcium channel blockers on the increase in intracellular calcium, measured with Fluo-3, induced by the application of 500 nM Aβ with a puffer pipette (indicated by a *horizontal line* in Fig. 6*A*). The concentrations of the blockers were 1 μM CNQX, 50 μM D-AP5, 1 μM conotoxin, 1 μM agatoxin, 3 μM nifedipine, and 100 μM Na7. The effects were normalized with respect to control ($p < 0.05$). *B*, result of lowering calcium influx using a nominally Ca^{2+} free solution or 1 mM EGTA on the early and chronic effects of Aβ on miniature current frequency from three independent experiments ($p < 0.05$). For these experiments, the neurons were exposed to Aβ alone or in the presence of 100 μM Na7. *C* and *D*, effect of Aβ-induced reduction on SV2 in the presence and absence of Na7, Na13, and Na15. The *bars* are mean ± S.E. from nine different neurons ($p < 0.05$).

DISCUSSION

Effects of Low Aβ Concentrations on Synaptic Transmission—Only recent studies have dealt with the action of Aβ at concentrations without overt neurotoxicity on synaptic properties (35). Although some debate still exists on whether Aβ can down-regulate specific components of synaptic transmission, several studies in rodent hippocampus showed that Aβ affected long term potentiation, NMDA- and AMPA-evoked currents (8, 36, 37). Furthermore, studies in transgenic animals revealed that overexpression of amyloid precursor protein reduced presynaptic proteins (36) together with complex brain functions. In addition, it was shown that micromolar concentrations of Aβ inhibited long term potentiation and NMDA-evoked currents (8). Based on all this evidence, it is now accepted that minute synaptic dysfunctions may represent the earliest signs of AD (35).

The present study, with low concentrations of Aβ, demonstrates a largely unrecognized action of Aβ as an inhibitor of presynaptic function. For instance, release of synaptic vesicles, as measured by real time imaging with FM1-43, was increased. Aβ also enhanced the frequency of miniature synaptic currents, without changes in the amplitude and kinetics of the postsynaptic currents, supporting a primary effect of Aβ on presynaptic release. Nevertheless, higher concentrations and longer exposure times with Aβ affected postsynaptic properties such as current amplitude and protein expression levels (Figs. 1 and 4). The effect of Aβ on cultured hippocampal neurons was clearly evident on AMPAergic transmission in agreement with other studies in hippocampal slices (38). Clear postsynaptic effects of Aβ were not evident and might be complicated by the concentration and the type of active species. Although the present study was done with a mixture of amyloid aggregates, most likely present in the aging brain, previous studies utilized an oligomer-rich preparation (8, 38).

Mechanisms of Aβ Action—Presynaptic vesicle fusion to the active zones is strongly dependent on the entry of extracellular calcium and subsequent activation of intracellular signaling and cytoskeleton remodeling (39). Consequently, the early increase in synaptic transmitter release by Aβ was associated with the rise in intracellular calcium, in agreement with previous studies on liposomes and clonal cell lines (21, 22). This increase might depend on voltage-gated calcium channels (40), AMPA receptors (38), NMDA receptors (8), or formation of calcium-permeable membrane pores (21, 22, 32, 41). Our data showed that antagonists for calcium channels, NMDA and AMPA receptors were unable to block the Aβ-induced increase in intracellular calcium, although it was blocked by Na7, a small peptide reported to block calcium influx, through the amyloid pore (34, 42). Noteworthy, the early and delayed effects of Aβ on synaptic transmission were also blocked by Na7, suggesting that these synaptic effects resulted as a consequence of pore formation and subsequent calcium influx. Interestingly, the experimental procedures used to block the early synaptic potentiation also inhibited the delayed synaptic failure, suggesting that they are linked. Finally, a significant dysfunction in calcium homeostasis with Aβ is in good agreement with several studies that related AD to ion alterations, with calcium being central to these mechanisms (43). However, the contribution of other ions such as copper, iron, or zinc to the mechanism behind Aβ synaptotoxicity cannot be ruled out (44). In fact, histidine 13 and 14 of the Aβ sequence, corresponding to key amino acids for the metal-binding site of this peptide, are also determinants for the Aβ pore permeability (45). In terms of a mechanism explaining the synaptic failure, we found that chronic Aβ reduced the number of total and docked synaptic vesicles in nerve terminals and

reduced the RRP demonstrated by the hyperosmotic sucrose solution (46, 47).

Structurally, synaptic vesicles are found in three pools: (i) RRP that correspond to docked vesicles in the active site ready to be released (although see Ref. 48), (ii) the recycling pool sensitive only to strong stimulations (24), and (iii) the reserve pool located at a distance from the active zone. Therefore, these new results strongly support the idea that Aβ affects RRP and recycling pools, directly apposed to the active zone.

Overall, we postulate that the earliest effects of low Aβ concentrations are mainly presynaptic and reflect a combination of disruption of RRP and recycling pools. Interestingly, these novel actions of Aβ show strong similarities, although with lower potency, to the effect of α-latrotoxin on neurotransmission. For example, after a strong enhancement of synaptic transmission, α-latrotoxin induced vesicle depletion and diminution in miniature potentials by a pore-forming mechanism (49), having conductance and kinetic properties very similar to those of pores formed by Aβ in lipid bilayers (50). The characterization of Aβ-induced calcium-permeable pores, displaying properties similar to those of α-latrotoxin, is currently under study in our laboratory.

Acknowledgments—We thank Dr. Ricardo Miledi for critically reading the manuscript and Lauren Aguayo for technical and editing assistance.

REFERENCES

1. Selkoe, D. J. (2002) *Science* **298,** 789–791
2. Mattson, M. P. (1997) *Physiol. Rev.* **77,** 1081–1132
3. McLean, C. A., Cherny, R. A., Fraser, F. W., Fuller, S. J., Smith, M. J., Beyreuther, K., Bush, A. I., and Masters, C. L. (1999) *Ann. Neurol.* **46,** 860–866
4. Shankar, G. M., Bloodgood, B. L., Townsend, M., Walsh, D. M., Selkoe, D. J., and Sabatini, B. L. (2007) *J. Neurosci.* **27,** 2866–2875
5. Goodman, L. S., Hardman, J. G., Limbird, L. E., and Gilman, A. G. (2001) *Goodman and Gilman's the Pharmacological Basis of Therapeutics*, pp. 203–220, 10th Ed., McGraw-Hill, New York
6. Oddo, S., Caccamo, A., Shepherd, J. D., Murphy, M. P., Golde, T. E., Kayed, R., Metherate, R., Mattson, M. P., Akbari, Y., and LaFerla, F. M. (2003) *Neuron* **39,** 409–421
7. Shankar, G. M., Li, S., Mehta, T. H., Garcia-Munoz, A., Shepardson, N. E., Smith, I., Brett, F. M., Farrell, M. A., Rowan, M. J., Lemere, C. A., Regan, C. M., Walsh, D. M., Sabatini, B. L., and Selkoe, D. J. (2008) *Nat. Med.* **14,** 837–842
8. Snyder, E. M., Nong, Y., Almeida, C. G., Paul, S., Moran, T., Choi, E. Y., Nairn, A. C., Salter, M. W., Lombroso, P. J., Gouras, G. K., and Greengard, P. (2005) *Nat. Neurosci.* **8,** 1051–1058
9. Nomura, I., Kato, N., Kita, T., and Takechi, H. (2005) *Neurosci. Lett.* **391,** 1–6
10. Chauhan, N. B., and Siegel, G. J. (2002) *J. Neurosci. Res.* **69,** 10–23
11. Reddy, P. H., Mani, G., Park, B. S., Jacques, J., Murdoch, G., Whetsell, W., Jr., Kaye, J., and Manczak, M. (2005) *J. Alzheimers Dis.* **7,** 103–117
12. Kelly, B. L., Vassar, R., and Ferreira, A. (2005) *J. Biol. Chem.* **280,** 31746–31753
13. Kelly, B. L., and Ferreira, A. (2006) *J. Biol. Chem.* **281,** 28079–28089
14. Ye, C., Walsh, D. M., Selkoe, D. J., and Hartley, D. M. (2004) *Neurosci. Lett.* **366,** 320–325
15. Glabe, C. G., and Kayed, R. (2006) *Neurology* **66,** S74–S78
16. Tapia, J. C., Mentis, G., Navarrete, R., Nualart, F., Figueroa, E., Sánchez, A., and Aguayo, L. G. (2001) *Neuroscience* **108,** 493–506
17. Ryan, T. A., Smith, S. J., and Reuter, H. (1996) *Proc. Natl. Acad. Sci. U.S.A.* **93,** 5567–5571
18. Walsh, D. M., and Selkoe, D. J. (2004) *Protein Pept. Lett.* **11,** 213–228
19. Wang, Q., Walsh, D. M., Rowan, M. J., Selkoe, D. J., and Anwyl, R. (2004) *J. Neurosci.* **24,** 3370–3378
20. Rhee, J. S., Ebihara, S., and Akaike, N. (1994) *J. Neurophysiol.* **72,** 1103–1108
21. Alarcón, J. M., Brito, J. A., Hermosilla, T., Atwater, I., Mears, D., and Rojas, E. (2006) *Peptides* **27,** 95–104
22. Demuro, A., Mina, E., Kayed, R., Milton, S. C., Parker, I., and Glabe, C. G. (2005) *J. Biol. Chem.* **280,** 17294–17300
23. Ryan, T. A., Reuter, H., Wendland, B., Schweizer, F. E., Tsien, R. W., and Smith, S. J. (1993) *Neuron* **11,** 713–724
24. Ryan, T. A., and Smith, S. J. (1995) *Neuron* **14,** 983–989
25. Yao, P. J., and Coleman, P. D. (1998) *Neurosci. Lett.* **252,** 33–36
26. Grace, E. A., Rabiner, C. A., and Busciglio, J. (2002) *Neuroscience* **114,** 265–273
27. Kriebel, M. E., and Pappas, G. D. (1987) *Neuroscience* **23,** 745–756
28. Lonart, G., and Simsek-Duran, F. (2006) *Brain Res.* **1107,** 42–51
29. Cousin, M. A., and Robinson, P. J. (2000) *J. Neurosci.* **20,** 949–957
30. Bobich, J. A., Zheng, Q., and Campbell, A. (2004) *J. Alzheimers Dis.* **6,** 243–255
31. Blanchard, B. J., Konopka, G., Russell, M., and Ingram, V. M. (1997) *Brain Res.* **776,** 40–50
32. Arispe, N., Pollard, H. B., and Rojas, E. (1994) *Ann. N.Y. Acad. Sci.* **747,** 256–266
33. Arispe, N. (2004) *J. Membr. Biol.* **197,** 33–48
34. Arispe, N., Diaz, J. C., and Simakova, O. (2007) *Biochim. Biophys. Acta* **1768,** 1952–1965
35. Haass, C., and Selkoe, D. J. (2007) *Nat. Rev. Mol. Cell Biol.* **8,** 101–112
36. Hsia, A. Y., Masliah, E., McConlogue, L., Yu, G. Q., Tatsuno, G., Hu, K., Kholodenko, D., Malenka, R. C., Nicoll, R. A., and Mucke, L. (1999) *Proc. Natl. Acad. Sci. U.S.A.* **96,** 3228–3233
37. Stéphan, A., Laroche, S., and Davis, S. (2001) *J. Neurosci.* **21,** 5703–5714
38. Hsieh, H., Boehm, J., Sato, C., Iwatsubo, T., Tomita, T., Sisodia, S., and Malinow, R. (2006) *Neuron* **52,** 831–843
39. Schneggenburger, R., and Neher, E. (2005) *Curr. Opin. Neurobiol.* **15,** 266–274
40. Ramsden, M., Plant, L. D., Webster, N. J., Vaughan, P. F., Henderson, Z., and Pearson, H. A. (2001) *J. Neurochem.* **79,** 699–712
41. Quist, A., Doudevski, I., Lin, H., Azimova, R., Ng, D., Frangione, B., Kagan, B., Ghiso, J., and Lal, R. (2005) *Proc. Natl. Acad. Sci. U.S.A.* **102,** 10427–10432
42. Qi, J. S., and Qiao, J. T. (2001) *Neuroscience* **105,** 845–852
43. Mattson, M. P., and Chan, S. L. (2003) *Cell Calcium* **34,** 385–397
44. Opazo, C., Huang, X., Cherny, R. A., Moir, R. D., Roher, A. E., White, A. R., Cappai, R., Masters, C. L., Tanzi, R. E., Inestrosa, N. C., and Bush, A. I. (2002) *J. Biol. Chem.* **277,** 40302–40308
45. Díaz, J. C., Linnehan, J., Pollard, H., and Arispe, N. (2006) *Biol. Res.* **39,** 447–460
46. Khvotchev, M., Lonart, G., and Südhof, T. C. (2000) *Neuroscience* **101,** 793–802
47. Rosenmund, C., and Stevens, C. F. (1996) *Neuron* **16,** 1197–1207
48. Rizzoli, S. O., and Betz, W. J. (2005) *Nat. Rev. Neurosci.* **6,** 57–69
49. Ashton, A. C., Volynski, K. E., Lelianova, V. G., Orlova, E. V., Van Renterghem, C., Canepari, M., Seagar, M., and Ushkaryov, Y. A. (2001) *J. Biol. Chem.* **276,** 44695–44703
50. Kourie, J. I., Henry, C. L., and Farrelly, P. (2001) *Cell. Mol. Neurobiol.* **21,** 255–284

β-Amyloid Causes Depletion of Synaptic Vesicles Leading to Neurotransmission Failure

Jorge Parodi, Fernando J. Sepúlveda, Jorge Roa, Carlos Opazo, Nibaldo C. Inestrosa and Luis G. Aguayo

J. Biol. Chem. 2010, 285:2506-2514.
doi: 10.1074/jbc.M109.030023 originally published online November 13, 2009
